# Optical Based Characterisation of an Aluminium Alloy

Y.H. Tai, D.T. Asquith, C. Pinna and J.R. Yates

SIRIUS, Department of Mechanical Engineering, University of Sheffield
Mappin Street, Sheffield S1 3JD, UK

mep04yht@sheffield.ac.uk

**Keywords**: Aluminium lithium, 2195, anisotropy, and digital image correlation

**Abstract.** Recent developments have meant the use of advanced materials such as aluminium-lithium alloys is increasingly common for weight critical applications, especially in the aerospace industry. Even though these alloys are in their fourth generation, some variants can be highly anisotropic and have poor fatigue and fracture properties. This paper will report on findings from mechanical and metallurgical testing that are based predominantly on optical techniques with emphasis on digital image correlation (DIC). The aim is to obtain a better understanding of the fracture process by means of integrating microstructure with mechanical properties. Results show that 2195 exhibits significant anisotropy in both tensile and tear tests. The alloy also exhibits crack propagation which follows unstable crack paths and is a cause for concern. Further work is being carried out to obtain data which will aid in the understanding of the fracture and fatigue properties with the aim of optimising material properties.

## Introduction

The use of advanced light weight materials such as aluminium-lithium alloys in weight critical applications such as aircraft is increasingly common. This is because these materials offer weight, stiffness and strength advantages over conventional aluminium alloys. However, aluminium-lithium alloys have been found to be highly anisotropic, and in certain variants, have reduced fatigue and crack propagation resistance. This has limited the use of the material.

This paper reports on findings from work done on 2195-T8. Standard mechanical characterisation methods, tensile and compact tension (CT) tear test, were used in conjunction with metallographic characterisation to obtain a better understanding of the material fracture properties. Data acquisition and measurements was based on optical techniques which have been shown to work better than conventional measurement techniques [1]. The optical method of choice was digital image correlation (DIC) because it is simple, robust and cost effective. Following this section will be a short introduction to the principles behind DIC and the system used in this study.

Parameters of interest in this study were microstructure characteristics, stress strain curves, crack path stability and tearing toughness. Due to the material's application, the crack tip opening angle (CTOA) fracture parameter was used as a measure of tearing toughness. This was due to previous work by other researchers [2] which show CTOA to be a promising approach for structural integrity assessments of low constraint structures. An illustration of CTOA is shown in Figure 1.

The basic hypothesis for the CTOA fracture criterion is: for a given material with sufficiently large tearing modulus and a degree of hardening, there is a clearly definable crack tip profile and CTOA [3]. The CTOA value obtained for the material in the stable phase of crack extension is then used in conjunction with numerical methods to predict the onset of tearing in a structure made from the same alloy.

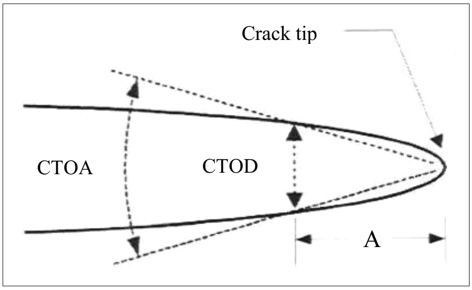


*Figure 1: Definition of CTOA and CTOD [4]*

## Digital image correlation

The principle of two-dimensional DIC is simple [5]. A digital image comprises a two-dimensional array of intensity values, $I(x,y)$. Given two images, $I_A$ and $I_B$, a $N \times N$ pixel region of interest, known as an interrogation window, is defined in each image. If the image brightness is approximately constant, $\sum I_A^2 \approx \sum I_B^2$, then a measure of the similarity between the two regions of interest can be expressed as a cross-correlation product [6]:

$$c(u,v) = \sum_{x=-m}^{n} \sum_{y=-n}^{n} I_1(x,y) I_2(x+u, y+v) \tag{1}$$

where $u$ and $v$ are the distances between the centres of the two regions of interest along $x$ and $y$ respectively, and $n$=$N$/2.

If $I_A$ is an image of some object and $I_B$ is another image of the same object after it has undergone some deformation or rigid body movement, then the maximum of the cross-correlation function (1) gives the most probable displacement values for the centre of the region of interest in $I_A$. In this work a commercial DIC package, DaVis 7 by LaVision, was used. In this implementation the images are first transformed into the frequency domain using a fast Fourier transform. Then the cross-correlation function equation 1 is calculated in the frequency domain. This proves to be several times faster than using equation 1 in the spatial domain [5].

## Experimental work

### *Material*

The material used in this study was an aluminium-lithium alloy 2195-T8 in 10 mm plate form. Composition analysis was performed and the results can be seen in Table 1 below. Lithium content is low but this is a normal feature of modern aluminium-lithium alloys.

*Table 1: Chemical composition of 2195 (wt %)*

| Ag | Zr | Fe | Cu | Ti | Mg | Li | Zn | Al |
|---|---|---|---|---|---|---|---|---|
| 0.28 | 0.11 | 0.03 | 3.83 | 0.02 | 0.36 | 1.02 | 0.02 | Balance |

### *Microstructure*

For microstructure characterisation, typical material cross-sections from three different faces of the plate were cold mounted in epoxy resin and polished using a fully automatic polishing machine (Phoenix 4000) using MetPrep 91 polishing guidelines [7]. It was then etched in Keller's reagent for one minute and cleaned with nitric acid to give good grain structure contrast. Subsequently, the cross-sections were analysed using a bright field optical microscope at various magnifications.

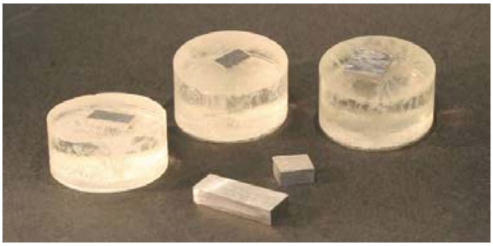

*Figure 2: Typical cross sections prior to and after cold mounting in epoxy resin*

### *Tensile test*

Standard tensile tests were performed to obtain the material stress strain curve. As the material was supplied in 10 mm plate form, the tensile specimens could be machined into round cross-section with a diameter in the gauge length of 8.0 mm. Having a circular gauge section meant that contraction data could be obtained as well. The specimens were cut from both L (along rolling direction) and TL directions (perpendicular to rolling direction) to determine the extent of material anisotropy. Figure 3 shows the prepared tensile specimens.


*Figure 3: Prepared tensile specimen*

Testing was done using a 100 kN electric machine (Mayes) fitted with appropriate grips to hold the specimens in place. The experimental set-up is shown in Figure 4. It was done under displacement control and displacement rate was set at 0.01 mm/s. The specimens were polished using fine emery paper prior to testing so that any surface imperfections which may influence the results were minimised. Measurements of the initial cross-section were also done for each specimen using a micrometer.

Displacement measurements were done using DIC and to facilitate this, a random pattern was needed on the surface of the specimens. To minimise problems caused by paint crazing, the surface was sprayed lightly with a combination of black and white acrylic based spray paint. This gave a good random speckle pattern which can be seen in Figure 3. In order to minimise problem caused by reflections from the surface of the specimen especially when out of plane deformation occurs, photographic dulling spray was applied prior to testing.

*Figure 4: Experimental set-up for tensile tests*

***Tear test***

For crack propagation and tearing toughness tests, thin sheet CT specimens were used. Specimen dimensions followed the guidelines found in the ASTM E2472 standard [8]. The specimen is shown in Figure 5. The specimens were 10.0 mm thick with in-plane dimensions of 100 x 100 mm. The specimens were machined from the plate in both TL (crack propagating along rolling direction) and LT (crack propagating across to rolling direction) configuration. The notch was machined by electrode discharge machining (EDM) and fatigue pre-cracking was carried out prior to testing to generate a sharp crack and minimise crack path instability at initiation. The final notch length including the fatigue crack gave a crack length ratio of 0.45. This allowed for approximately 20.0 mm of geometry independent crack extension.

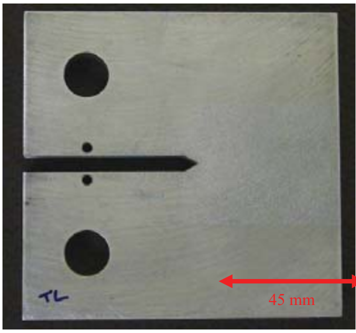


*Figure 5: CT specimen with speckle pattern on surface*

The experiment was carried out in the same electric Mayes test machine under quasi-static mode I loading conditions. Bespoke grips had to be manufactured to prevent any buckling or twisting of the specimen during the test. Displacement rate was set at 0.05 mm/s. Figure 6 below illustrates the experimental set-up. Data acquisition was done using a single computer running the DIC software logging data from all parameters of interest which allowed correlation between the measured parameters. Images were obtained at a rate of 1.0 Hz which was more than adequate for the intended purposes.

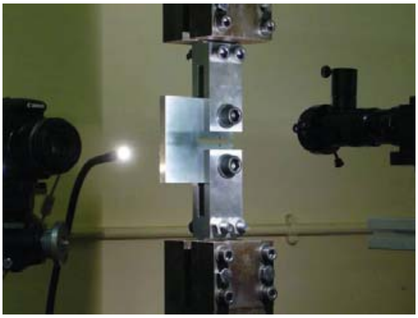

*Figure 6: Experimental set-up for tear tests*

DIC was used to give a measure of the surface displacements which were then used to calculate CTOA. Similar to the tensile test, a random pattern was created on the surface using the same techniques and the resultant pattern can be seen in Figure 5. The displacement fields around the propagating crack measured by DIC are illustrated in Figure 7 from which CMOD values were obtained to calculate CTOA using equation 2.

$$CTOA_{\theta} = 2\tan^{-1}\frac{CMOD}{A} \qquad (2)$$

Where, $A$ = distance from crack tip to measurement position

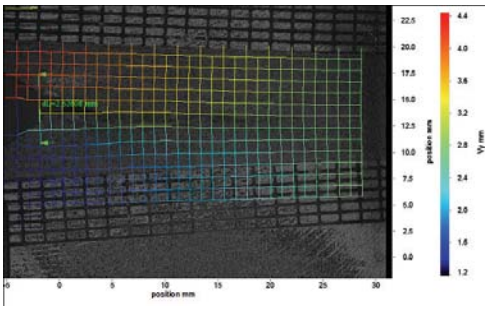


*Figure 7: Illustration of displacement fields on CT specimen surface*

**Results and discussion**

Microstructure characterization showed that this variant of 2195 has a highly directional grain structure. In the rolling (L) direction the grains appear long and thin. The average size of grains is approximately 500 µm by 12 µm by 10 mm. This suggests the material has been heavily rolled and should exhibit significant anisotropic behaviour. Figure 8 shows the results obtained from the metallographic study.

Results from the tensile tests show that the material does exhibit significant anisotropy as illustrated by the stress strain curves in Figure 9 below. Mechanical properties of the material were measured and calculated using DIC. The values are listed in Table 2 below. Accuracy of DIC has been shown before to be on par with conventional measurement techniques [9] and the results were also comparable with data from literature [10].

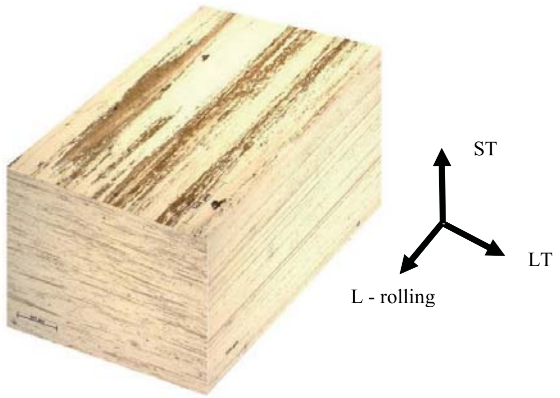


*Figure 8: Microstructure showing grain size and orientation*

*Table 2: Tensile test results for 2195-T8*

| Direction | Yield Strength 0.2%(MPa) | Tensile Strength (MPa) | Elongation (%) | Contraction (%) |
|---|---|---|---|---|
| L | 580 | 600 | 10.0 | -16.1 |
| TL | 525 | 550 | 8.0 | -22.8 |

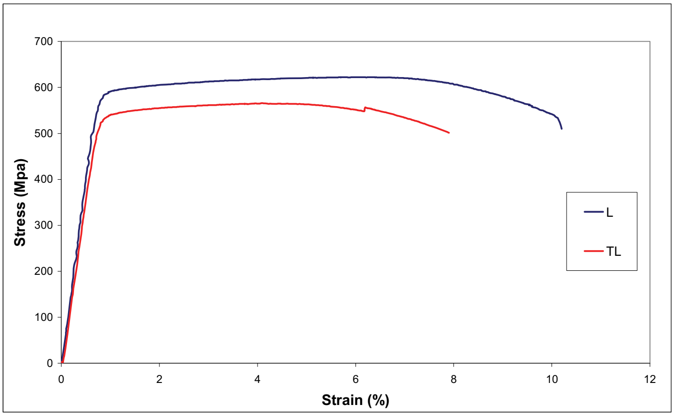


*Figure 9: Stress strain curve for 2195-T8 in L and TL directions*

The anisotropic behaviour the material's mechanical properties gave a good indication of the anisotropic properties to be expected in the tear test. Figure 10 shows the fractured CT specimens in both LT and TL directions with the corresponding fracture surface. In the LT direction, the crack path was highly unstable and there was sufficient evidence from analysing the fracture surface to suggest severe crack tunnelling. Mode of fracture can be considered a combination of flat fracture in the middle and shear fracture on either side. Shear lips near the surface also suggest slippage along the grain boundaries of the thin and highly directional grains. Further analysis of the fracture surface is needed to better understand the cause of the instability.

For the specimen in the TL direction, the fracture surface indicated predominantly flat fracture throughout the fracture process. There was also no evidence of crack tunnelling. Stability of the crack path was good but resistance to cracking was low in comparison. Experimental data also showed evidence of sudden crack extension followed by a short hardening stage in intermittent stages throughout the fracture process. Further analysis is needed to ascertain the significance and cause of this phenomenon.

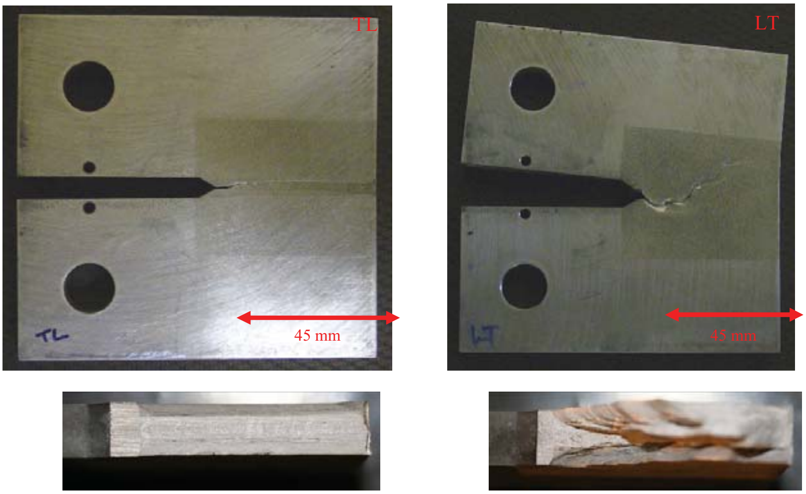


*Figure 10: Fractured CT specimens*

Fracture toughness results using CTOA as the measure also showed this material to be substantially tougher in the LT direction. In the stable region, the average value of CTOA obtained in the LT direction is 7.60° deg and the average value for CTOA in the TL direction is 3.00° deg. This shows that the tearing toughness in LT direction is at least twice that of the TL direction. The CTOA resistance is shown Figure 11. However, based on the guidelines in the ASTM E2472 standard [8], the results in the LT direction should be deemed invalid for integrity assessments because the crack path has deviated more than 10.0 degrees from the intended path and therefore changing the level of constraints. Nevertheless, as measure of fracture toughness, the results can still be considered to be useful.

The results from all three characterisation methods has shown that this form of 2195-T8 is highly anisotropic. It would be appropriate to say that as a structural material, it has good strength and weight for an aluminium alloy. However, the highly anisotropic fracture properties and crack path instability means that any particular structure has to be well designed to take into account these properties. There is still more scope for improvement and it hoped that further analysis of the results and microstructure will give a better idea of parameters which can be optimised to produce a material with improved properties.

Based on the results obtained from both tensile and tear test, the optical measurements have shown to be reliable and accurate. Significantly more data can be obtained using these techniques and it has also simplified the experimental procedure. There is certainly scope to further develop the use of these techniques.

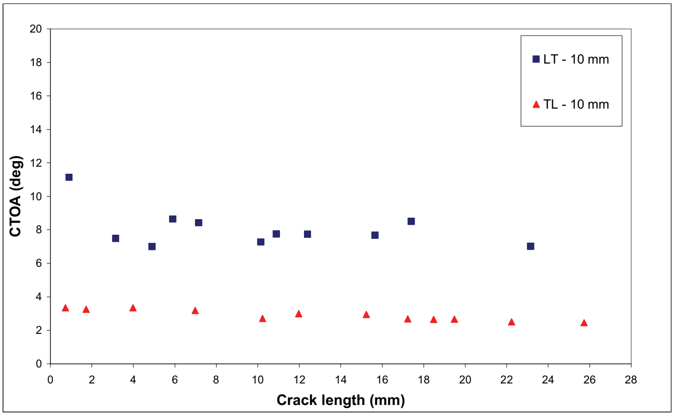


*Figure 11: CTOA resistance curve*

## Final comments

Results have shown 2195 to be an aluminium lithium alloy with highly anisotropic properties. Further work is needed to understand the cause of the anisotropy and how it can be improved upon. Optical characterisation has worked well for the experiments performed.

## References

(1) Tai Y H, López-Crespo P, Ayvar-Soberanis S, Yates J R, Shterenlikht A, Patterson E A, and Withers P J. *Optical Experimental Methods for Determining Fatigue and Fracture Properties*. in *Fatigue 2007*. 2007. Queen's College, Cambridge

(2) Newman J C Jr, James M A, and Zerbst U (2003) *A Review of the CTOA/CTOD Fracture Criterion*. Engineering Fracture Mechanics **70**, 371 - 385

(3) Barnby J T, Nadkarni A S, and Cresswell S L, *Experimental Determination of Crack Tip Angles (CTOA) and their Applicability to Instability Prediction in Structures.* International Journal of Materials and Product Technology, 1995. **10** (1): p. 161-170.

(4) Mahmoud S and Lease K (2003) *The Effect of Specimen Thickness on the Experimental Characterization of Crtical Crack-Tip-opening Angle in 2024-T351 Aluminium Alloy*. Engineering Fracture Mechanics **70**, 443 - 456

(5) Da Fonseca J Q, Mummery P M, and Withers P J (2005) *Full-field strain mapping by optical correlation of micrographs acquired during deformation*. Journal of Microscopy **218 (1)**, 9 – 21

(6) Clocksin W F, Quinta da Fonseca J, Withers P J, and T. P. H. S (2002) *Image processing issues in digital strain mapping*. In Proceedings of SPIE **4790**, 384 - 395

(7) MetPrep, MetPrep Procedure 91, www.metprep.co.uk

(8) ASTM-E2472 (2006) *Standard Test Method for Determination of Resistance to Stable Crack Extension under Low-Constraint Conditions*.

(9) Tai Y H, Asquith D T, and Yates J R. *Optical Characterisation of Failure Mechanics in an Aluminium-Lithium Alloy*. in *ICEI 2007*. 2007. UTeM, Malaysia

(10) Johnston W M, Pollock W D, and Dawicke D S (2002) *Biaxial Testing of 2195 Aluminum Lithium Alloy Using Cruciform Specimens.*NASA/CR-2002-211942